Mapping Height and Biomass of Mangrove Forests in Everglades National Park with SRTM Elevation Data

Marc Simard, Keqi Zhang, Victor H. Rivera-Monroy, Michael S. Ross, Pablo L. Ruiz, Edward Castañeda-Moya, Robert R. Twilley, and Ernesto Rodriguez

Abstract

We produced a landscape scale map of mean tree height in mangrove forests in Everglades National Park (ENP) using the elevation data from the Shuttle Radar Topography Mission (SRTM). The SRTM data was calibrated using airborne lidar data and a high resolution USGS digital elevation model (DEM). The resulting mangrove height map has a mean tree height error of 2.0 m (RMSE) over a pixel of 30 m. In addition, we used field data to derive a relationship between mean forest stand height and biomass in order to map the spatial distribution of standing biomass of mangroves for the entire National Park. The estimation showed that most of the mangrove standing biomass in the ENP resides in intermediate-height mangrove stands around 8 m. We estimated the total mangrove standing biomass in ENP to be 5.6 $\times$ 10^9 kg.

Introduction

Mangroves are salt tolerant trees located along tropical coasts. The mangrove forest acts as a buffer between land and sea reducing the impact of storm surge, waves, and erosion of the shore (Badola and Hussain, 2005). Mangrove ecosystems are among the most productive on Earth with a mean production of 2.5 g C m^{-2} day^{-1} (Jennerjahn and Ittekkot, 2002), and they contribute 11 percent of global total export to the ocean. Mangroves have experienced significant worldwide loss due to urbanization, exploitation, and sea level rise. Evaluating the spatial distribution and areal extent of mangroves in coastal margins has been a research priority since the 1970's due to the significant reduction in area as result of human and natural disturbances (Spalding *et al.*, 1997; Rivera-Monroy *et al.*, 2004). It is estimated that about 35 percent of the global area of mangroves has been lost during the last 20 years, a rate of reduction that exceeds that of other tropical ecosystems such as coral reefs and rain forests (Valiela *et al.*, 2001; Alongi, 2002). The use of satellite imagery to monitor mangrove distribution has advanced rapidly in recent years, allowing the determination of forest structural properties ranging from species-specific distribution (e.g., Wang *et al.*, 2004) to leaf area index (e.g., Kovacs *et al.*, 2005). However, few studies have attempted to estimate structural properties related to tree height or biomass at the landscape level (e.g., Mougin *et al.*, 1999). Landscape level estimates of mangrove biomass are needed because of the importance of mangroves in the carbon cycle of tropical coastal systems. Mangrove forests are usually characterized by sediment accretion (Lynch *et al.*, 1989; Woodroffe, 1992) which, combined with their high productivity and low ratio of sediment respiration to net primary production, enhances the potential for long-term sequestration of organic carbon (Twilley *et al.*, 1992; Jennerjahn and Ittekkot, 2002; Gonneea *et al.*, 2004). The global storage of carbon in mangrove biomass is estimated at 4.03 Pg; 70 percent of which occurs in coastal margins from 0° to 10° latitude (Twilley *et al.*, 1992).

Most research on mangroves is performed in small plots that are relatively easy to access. The study of large mangrove forests within the context of adjacent ecosystems (i.e., landscape scale) requires the use of maps. Remote sensing technology enables large area surveys and has been used in several studies to understand mangrove forests at the landscape scale. Several studies have shown that SPOT and Landsat imagery allow the distinction of mangroves from other cover types, though discrimination can be site specific and distinction of various mangrove species is not always clear with optical sensors (Ramsey and Jensen, 1996; Laba *et al.*, 1997; Rasolofoharinoro *et al.*, 1998; Aschbacher *et al.*, 1995). On the other hand, Lucas *et al.* (2000) used aerial stereo-photography to measure tree height and study mangrove succession. However, this method is limited by the availability and spatial coverage of the data. Promising investigations using radar remote sensing technologies were used to study hydrology in Everglades National Park (ENP) (Wdowinski *et al.*, 2004; Kasischke *et al.*, 2003; Bourgeau-Chavez *et al.*, 2005), though they did not address mangroves

Marc Simard and Ernesto Rodriguez are with the Radar and Engineering Section, Caltech-Jet Propulsion Laboratory, MS 300-319D, 4800 Oak Grove Drive, Pasadena, CA 91109 (marc.simard@jpl.nasa.gov)

Keqi Zhang is with the International Hurricane Research Center & Department of Environmental Studies, Florida International University, 11200 SW 8th St., Miami, FL 33199.

Victor H. Rivera-Monroy, Edward Castañeda-Moya and Robert R. Twilley are with the Wetland Biogeochemistry Institute, Department of Oceanography and Coastal Sciences, Louisiana State University, 3209 Energy, Coast & Environment Bldg., Baton Rouge, Louisiana 70803.

Michael S. Ross and Pablo L. Ruiz are with the Southeast Environmental Research Center, Florida International University, 11200 SW 8th St., Miami, FL 33199.

Photogrammetric Engineering & Remote Sensing
Vol. 72, No. 3, March 2006, pp. 299–311.

0099-1112/06/7203–0299/$3.00/0

directly. High correlations between radar data and structural parameters (e.g., tree density, basal area, height, diameter at breast height (DBH), biomass, age, and their distributions within forests) have been observed (Proisy *et al.*, 1996; Aschbacher *et al.*, 1995; Held *et al.*, 2003). In certain cases, the use of radar data allows for the delineation of flooding zones under mangrove forest canopies, though this capacity is limited at higher forest standing biomass (Proisy *et al.*, 2000) due to canopy attenuation and/or the presence of pneumatophores and aerial roots (Wang and Imhoff, 1993; Held *et al.*, 2003; Simard *et al.*, 2000). Models to identify scattering mechanisms and estimate mangrove physical parameters directly have also been developed (Proisy *et al.*, 2000; Wang and Imhoff, 1993). Mougin *et al.* (1999) found that radar penetrates only a few meters into the canopy and that backscatter saturates in mangrove stands of biomass greater than 160 Mg/ha. However, mapping of the vertical structure of mangroves at the landscape scale is still needed. One of the reasons for this lack of information is that mangrove forests are particularly difficult to survey due to the high density of trees and roots, as well as the extent of tidal channels and permanently or tidally flooded land surface.

The Shuttle Radar Topography Mission (SRTM) elevation data is available with high spatial resolution (30 m) throughout the U.S. These data can be used to determine the significance of mangrove forest as carbon sinks by relating tree height to available ground estimates of mangrove forest biomass at local scales, particularly since mangrove tree height is a good indicator of forest biomass (Cintron and Schaeffer-Novelli, 1984). However, radar estimates of mean tree height data must be calibrated. Recent emerging airborne light detection and ranging (lidar) technology provides an ideal tool to calibrate radar data since the tree height data can be derived directly from lidar measurements. Airborne lidar systems are capable of measuring objects on the earth surface with a horizontal resolution of several meters and centimeter vertical accuracy (Hyppa *et al.*, 2004). The combination of information at different spatial scales will aid in quantifying the functional role of coastal forested wetlands in tropical regions, and in understanding their contribution to the global carbon budget.

The objective was to produce a map of mangrove forest height in Everglades National Park (ENP) at the landscape scale with SRTM C-band elevation data. We calibrated SRTM mean tree height estimates with lidar data and a high-resolution DEM available for ENP (Desmond, 2003) (USGS/Southern Florida Information Access, SOFIA). We also show how we use the landscape scale map of mangrove height in conjunction with field data to estimate the standing biomass of mangroves.

The Test Site: Everglades National Park

Mangrove forests of south Florida are an ideal site to study the impact of sea level rise, hurricane activity, and urbanization on the structural and functional properties of coastal wetlands. The mangroves of south Florida are mainly located inside national parks and other protected areas, and therefore are protected from the direct impact of urbanization (Figure 1). However, hydrological changes in the last 100 years have significantly impacted the Everglades (Light and Dineen, 1994; Sklar *et al.*, 2002). During this period, canals and levees built for agricultural purposes and flood protection have segmented the upper Everglades watershed reducing water flow such that wetlands downstream receive surface water mainly as point-source inputs at canal structures. This reduction in freshwater flow has increased salinity in adjacent estuaries, such as Florida Bay (McIvor

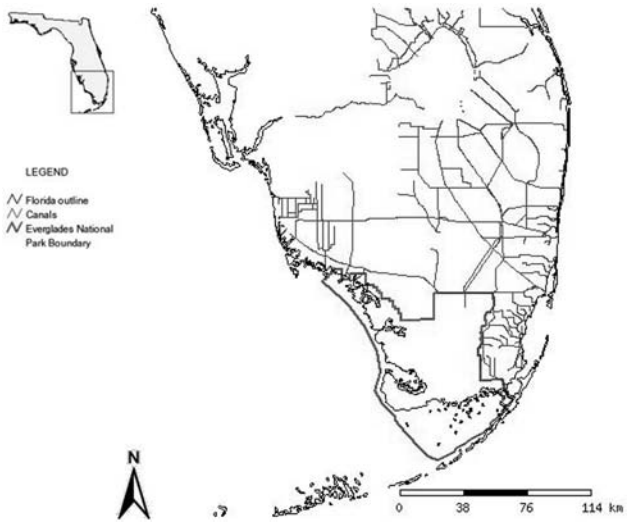

Figure 1. Everglades map showing the location of the Everglades National Park in Southern Florida with the current canals. The city of Miami is located on the eastern side of the ENP. (Marc Simard using the "Florida Coastal Everglades LTER Mapserver Project", URL: **http://fcelter.fiu.edu/gis/everglades-map/**).

et al., 1994; Rudnick *et al.*, 1999). As a result of this freshwater reduction and increasing salinity in south Florida, plant communities are changing in species composition and spatial distribution. Currently, there is an increasing abundance and dispersion inland of more marine and brackish species, which are more tolerant to salt. One example of this replacement is the migration of scrub mangrove forests in the southeast Taylor region and Biscayne Bay. The freshwater reduction combined with a 2.0 mm annual sea level rise led to a 3.5 km landward migration of mangrove zones since the 1940's in southeast Taylor slough (Ross *et al.*, 2000). Sea level rise and its potential acceleration with global warming threaten to push mangrove forests further landward.

The U.S. government has allocated 7.8 billion dollars for restoring the ecosystems of the Everglades (CERP, 2000). It is expected that the ongoing restoration project will increase the quantity, quality, and timing of fresh water reaching the Florida coast and among other objectives slow down or even reverse the landward migration of the mangroves in some locations. This process is further complicated by entry into a period of more frequent hurricanes due to the decadal change of storm activity (Smith *et al.*, 1994; Davis *et al.*, 2004). In order to document the impact and success of the Everglades restoration project, the current spatial distribution and productivity of mangrove forests in the region must be recorded to establish a baseline for future comparisons.

Data Description

We used several datasets including some that are distributed freely through the Internet, i.e., (a) a land-cover map of the Everglades, (b) a high-resolution Digital Elevation Model (DEM), and (c) the SRTM elevation data. The lidar and field data were acquired specifically for this project. We describe these datasets in the following paragraphs.

Land Cover Map

In this work, we used a vegetation map produced by the Center for Remote Sensing and Mapping Science (CRMS) of

the University of Georgia (UG) (Vegetation Map, 1999; PE&RS Special Issue, 1999; Welch and Madden, 1999). This map is the product of a collaborative effort by the National Park Service South Florida Natural Resources Center at ENP, CRMS, and the South Florida Water Management District. A complete GIS vegetation database of the Everglades was produced using color-infrared (CIR) aerial photographs. The overall land-cover classification accuracy is 85 percent. We used this map to delineate and isolate the mangroves within the ENP by merging all mangrove classes (see Table 1) and built a mangrove mask (Plate 1). The estimated total area of mangroves in the ENP was 144,447 ha.

TABLE 1. COMPOSITION OF ENP MANGROVE MASK: THE MANGROVE LAND-COVER CLASSES OF UNIVERSITY OF GEORGIA LAND-COVER MAP WERE MERGED INTO A SINGLE POLYGON

UG Map Labels	Class
M	Mangrove Forest
FMa	Black Mangrove(Avicennia Germinans)
FM1	White Mangrove(Laguncularia Racemosa)
FM1b	White Mangrove or Buttonwood Forest
FMr	Red Mangrove (Rhizophora mangle)
FMx	Mixed Mangrove
FB	Buttonwood (Conocarpus erectus)
SM	Mangrove Scrub
SMr	Red (Rhizophora mangle)
Sma	Black (Avicennia Germinans)
SM1	White (Laguncularia Racemosa)
SM1b	White Mangrove or Buttonwood Scrub
SMx	Mixed scrub (Sparse and high density)
SC	Buttonwood Scrub (Conocarpus Erectus)

The Digital Elevation Model

The USGS/SOFIA DEM (Desmond, 2003) (Figure 2a) is a high resolution DEM built to model sheet flow of water over the extremely low relief terrain of south Florida and was produced by interpolating thousands of field data points on a 400 m grid pattern with a specification of 15 cm elevation accuracy. However, experiments have shown the mean difference between the DEM and the NGS first-order benchmarks (relative to NAVD88, the North American Vertical Datum) was only 3.3 cm.

SRTM Elevation Data

In February 2000, STS-99 successfully fulfilled its SRTM mission and gathered elevation data over 80 percent of the land surfaces of the Earth. The objective of SRTM was to map the topography of the Earth's land surface on a global scale by radar interferometry. Interferometry uses interference patterns between two radar signals in order to derive terrain height. Space Shuttle Endeavour was equipped with two radar antennas separated by a 60 m boom (baseline) operating at C-band and X-band. The interference occurs because the signal

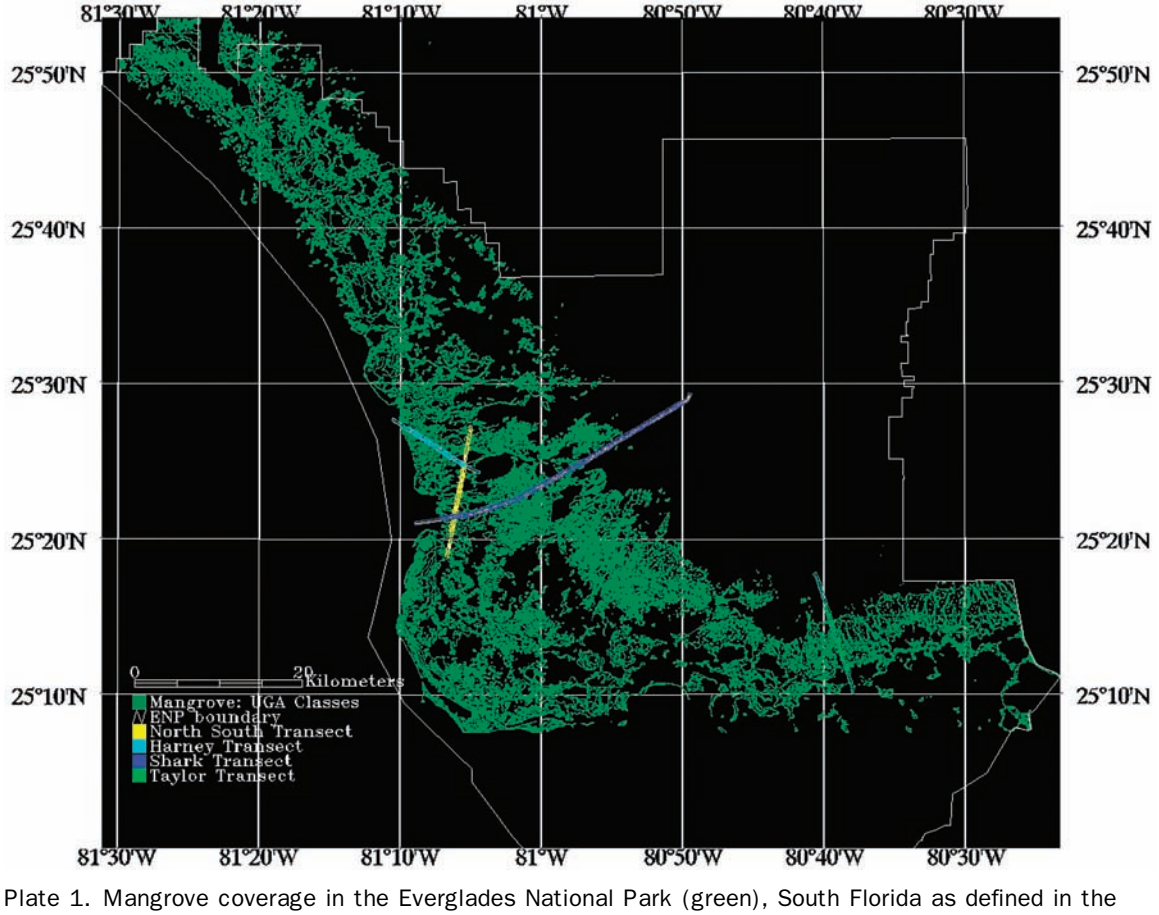

Plate 1. Mangrove coverage in the Everglades National Park (green), South Florida as defined in the land cover map of the Everglades produced by University of Georgia's Center for Remote Sensing and Mapping Science, South Florida Natural Resources Center, and the Everglades National Park. The plate also shows the ENP boundary and the four lidar transects collected to calibrate SRTM elevation data.

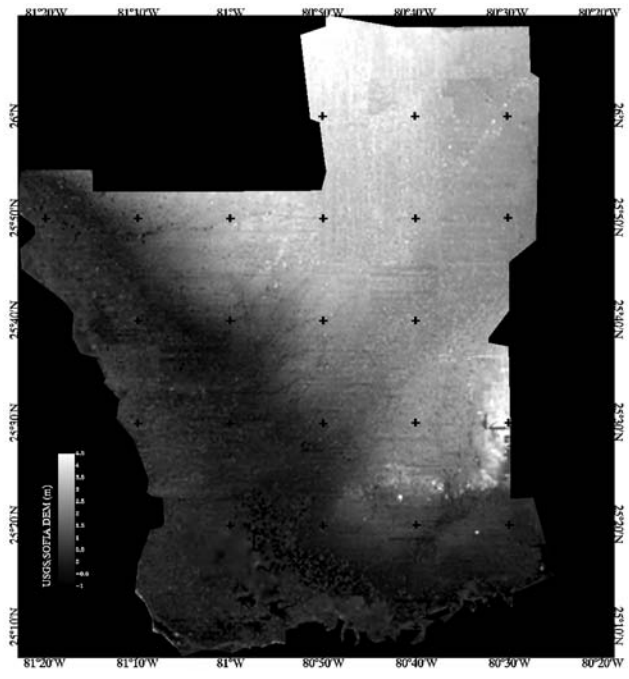

(a)

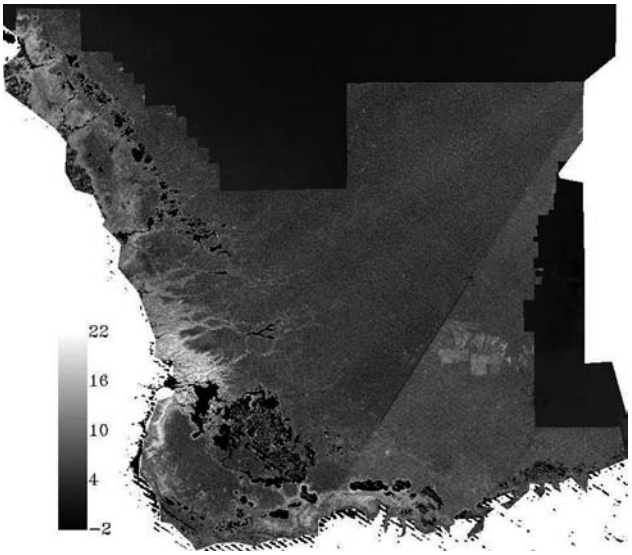

(b)

Figure 2. (a) USGS/SOFIA DEM with a ±15 cm elevation difference accuracy. The USGS coordinated the acquisition of high accuracy elevation data. The elevation data was collected on a 400 by 400 meter grid that we translated to WGS84 Datum using RSI's ENVI® software; (b) Difference image between SRTM elevation data and USGS DEM. We fitted a plane through the southeast to subtract 2 m.

from a given point on the Earth surface returns with a different phase to the antenna. This difference can be translated into a terrain height estimate. The near-global topographic maps of the Earth (called Digital Elevation Models or DEM's) were made from the C-band radar data and were processed at the Jet Propulsion Laboratory (Hensley *et al.*, 2000). During ground processing all information related to radar polarization (HH and VV polarization) and temporal changes that may have occurred between SRTM passes (e.g., tides) were lost during averaging. SRTM interferometric C-band data provides a unique global snapshot of mangrove wetlands. We used the SRTM-1 data format available in 16-bit signed integer format conveniently referenced to the WGS84 and EGM96 Geoid. SRTM X-band data did not cover the mangroves of the ENP.

Radar scattering occurs throughout the vegetation canopy and the measured height is located at the interferometric phase center. SRTM elevation data has a specified 16 m absolute error (90 percent Linear Error), however research has shown that when used in conjunction with other topographic data sets, SRTM elevation data can be used to estimate mean tree height with only a few meters of error (Kellndorfer *et al.*, 2004; Walker *et al.*, 2004). Kellndorfer *et al.* (2004) also found the scattering phase center to lie about 6 m below the mean observed stand height for slash pine plantations and around 1 m below mean height for mixed coniferous forests in California.

In this paper, we focus on mangroves which are located in the tidal region along the tropical coasts, and therefore we can in principle use the height relative to mean sea level to estimate canopy height. This measure is possible because the topographic elevation under the mangrove canopy is close to sea level. In the mangroves of south Florida, the topography fluctuates by less then 2 m (Figure 2a) and the tidal range is approximately 30 cm.

Lidar Data

Airborne lidar data were collected using an Optech ALTM 1233 system operated by Florida International University on 15–16 April and 14–16 May 2004. With a flight altitude of 500 m above the ground, flight speed of 210 km/hr, field of view angle of 40°, and pulse rate of 33 kHz, a 360 meter-wide swath of 13 cm wide laser footprints spaced approximately every 1.5 m beneath the flight path was produced. The locations of lidar survey transects are shown on Plate 1.

Airborne lidar systems obtain measurements for the horizontal coordinates (x, y) and elevation (z) of the reflective objects scanned by the laser beneath the flight path. These measurements generate a 3-dimensional cloud of points with irregular spacing. The laser-scanned objects for our transects mainly include vegetation and "bare ground." The canopy heights can be derived by subtracting the elevations of "bare ground" from those for canopy. In order to obtain the ground elevation, measurements from ground and vegetation must be separated. A progressive morphological (PM) filter (Zhang *et al.*, 2003) was used to extract ground points from the lidar data as described below.

Both first and last return measurements were collected by the system. Since the last returns most likely reached the ground, the last return data were used to extract ground points. A digital terrain model (DTM) was produced from identified ground points using Kriging interpolation. A digital surface model (DSM) was generated by interpolating first return data to estimate the canopy elevations because the first returns were more likely to have hit the top of the canopy. A canopy height grid was produced by subtracting the DTM from DSM. We show examples of height images in Figure 3.

Canopy height error (RMSE) as well as underestimation by lidar is generally less than 1 m (Hyyppa *et al.*, 2004). In our case, we derived a RMSE of 10 cm by comparing the elevations of 260 GPS measurements along 9.2 km road surface in the park with elevations of corresponding grid cells. A grid with a resolution of 1 m × 1 m was interpolated for RMS error estimation by applying the Kriging method to raw lidar measurements.

For SRTM calibration purposes, we filtered the elevation data with a 31 × 31 mean filter (i.e., 30 m × 30 m area) and

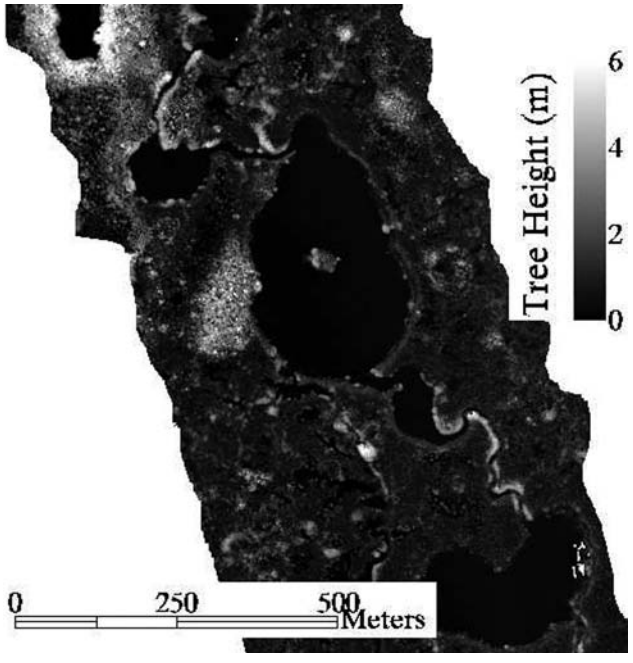

(a)

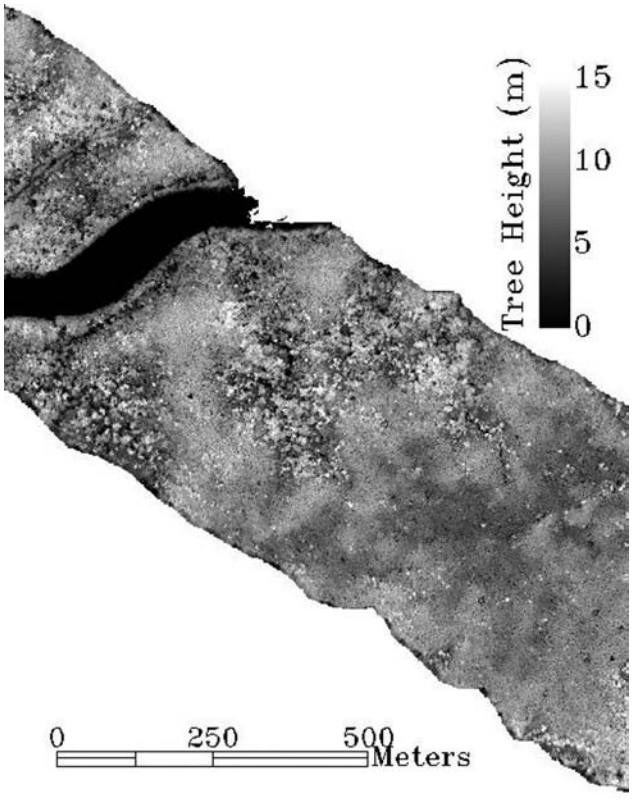

(b)

Figure 3. Example of lidar data collected over the Taylor Slough (a). This region is mainly characterized by short mangrove less then 2 m and spatially distributed as patches. (b) A lidar transect across the Harney River (northwest). The mangroves are much taller (>15 m, white on image).

co-registered the lidar data with the SRTM map with nearest neighbor interpolation. The co-registration also showed that the SRTM map has a sub-pixel geolocation error.

Field Data

We collected field data in order to estimate biomass in ENP. We used the variable plot method to sample the tree layer, with fixed nested plots for shrub and herb layers. This allowed us to determine a number of forest structural parameters to field truth portions within the lidar transects. However, we were unable to obtain accurate geolocation for our sampling points because of weak GPS signal under the canopy. The variable plot sampling has the advantage that the probability of tree selection is proportional to basal area, causing sparsely distributed large diameter trees to be sampled with the same intensity as denser, small diameter trees. The following stand-level structural characteristics were estimated: total tree basal area, tree density by species, height, diameter at breast height (DBH) and species composition, as well as tree seedling density. In variable plot sampling, each tree's plot size is dependent on its diameter, and trees are tallied as "in" or "out" of the plot depending on whether their diameter at breast height is large enough to subtend a fixed critical angle visible using a wedge prism or angle gauge from the plot center. "In" trees were tallied, with total basal area equaling the count of "in" trees times the basal area factor (BAF) of the prism. By measuring the DBH of each "in" tree, we could also calculate the density of trees in each size class (Grosenbaugh, 1952). We measured a total of 22 points over approximately 2.4 km for a total of 289 trees. In addition we used data from two sets of plots in scrub mangrove forest (canopy height 2 to 3 m or less) in Biscayne National Park and one scrub forest in Taylor Slough, ENP, in order to incorporate biomass estimates across the entire range of mangrove canopy heights.

At each point we also measured the height of each tree using a laser range finder. We assumed a user standard error of 10 percent in height measurement due to user reading and interpretation. Indeed, the tree top as seen from the ground may vary slightly depending on the interpreter's position, such that the height measurement of a tall tree (e.g., 20 m) varied by about 2 m. We used the field measurements solely to compute a relationship between stand mean tree height and biomass. To calibrate SRTM elevation, we used the lidar canopy height estimates as the true canopy height since the lidar error is smaller than field measurements.

During the field campaign, we were able to validate the 100 percent accuracy of the ENP mangrove mask (i.e., UGA land-cover map after merging mangrove classes of Table 1) for the visited mangroves sites: the Lostman's River, the Harney River, and Shark River. However, we could not validate the accuracy of the mask for the scrub mangrove forests which were generally located further inland.

SRTM Calibration Methodology

In this section, we discuss the methodology used to calibrate the SRTM estimates of mangrove height in terms of the USGS DEM and lidar. The calibration involves verification that the SRTM elevation data paralleled the DEM over grassland/bare ground. Secondly, we tested the SRTM elevation data for bias using mean sea level, and the lidar data is used to calibrate the mean tree height. We also discuss how the field data was combined with the SRTM mean tree height estimation to derive biomass at the landscape scale.

Calibrating SRTM Ground

We calibrated the SRTM elevation data in terms of ground elevation. We used two references: the USGS/SOFIA DEM

(Desmond, 2003) shown in Figure 2a and an SRTM mean sea level estimate. The elevation difference image shown in Figure 2b was produced by converting the projection and subtracting the DEM from SRTM data. The image shows that SRTM overestimated the ground by several meters. The image also includes an artifact in the SRTM DEM that coincides with the orientation of ascending passes, and results in an additional overestimation in the southeast corner. Using several polygons within the grassland region, we estimated a mean difference of 2.7 m between SRTM and the USGS DEM, while the mean difference in the southeast region was 4.7 m, with a standard deviation of 1.3 m. This indicates the additional overestimation in the southeast region was 2.0 m. In order to eliminate this discrepancy, we subtracted a flat plane of 2.0 m from the southeast corner that follows a clearly visible pattern (i.e., along the black arrow in Figure 2b). We refer to this "leveled" SRTM DEM as SRTM-L. The residual overestimation of ground elevation in SRTM-L is 2.7 m. However, in most of ENP area, the ground is covered by water, thick grasses, and sparse shrubs that may reach 2.5 m and may contribute to the SRTM-L ground elevation measurement. Since we did not have any bare ground data to identify possible SRTM-L elevation bias, we estimated mean sea level in a series of polygons in the coastal portions of ENP, including a total of 200,000 SRTM-L elevation points. We avoided no-value data points which are numerous over the sea, and most likely result from low radar backscatter and interferometric correlation. Mean sea level height was estimated at 1.1 m with a standard deviation of 2.8 m. This large estimation error is due to thermal noise, which is significant in low backscatter targets, such as water. If mean sea level as estimated with SRTM-L is considered as the bare ground elevation reference (i.e., vegetation height = 0) for mangroves, then SRTM-L overestimates elevation by +1.1 m. Considering the difference image of Figure 2b with a mean difference of 2.7 m, we concluded that the grasslands contribute the remaining 1.6 m. We neglected the 30 cm tide because its temporal signature was lost during the SRTM averaging process when averaging all passes. This averaging included up to three passes of different polarization, incidence angle, and acquisition time.

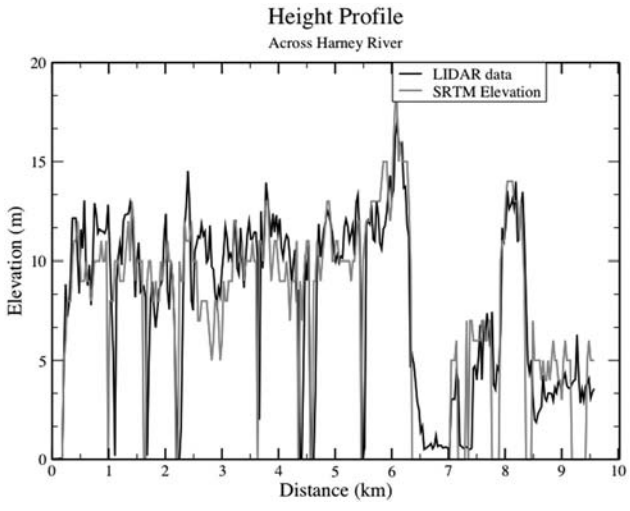

(a)

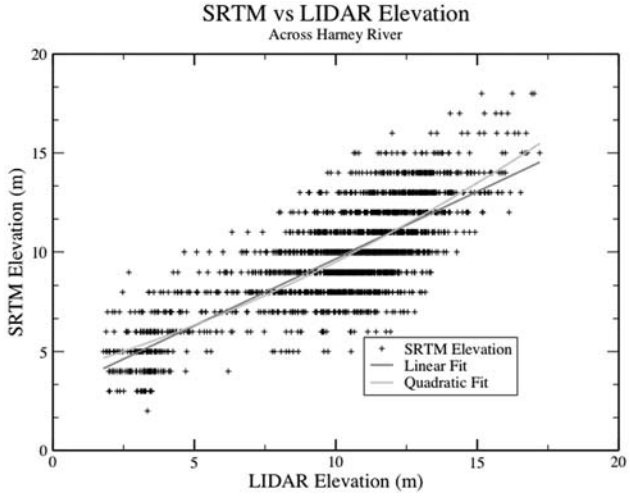

(b)

Figure 4. Transect across the Harney River: (a) Elevation profile for the lidar and SRTM data along the transect going toward the northwest. The profile is single valued at each point and therefore may not be representative of local statistics. The SRTM elevation data is higher then the lidar data toward the end of the Transect. This region is characterized by scrub mangroves and also grasses. (b) SRTM-L elevation versus lidar elevation. We fitted a linear and a quadratic regression curve given in Table 1 with a 79 percent correlation.

Mean Vegetation Height

The SRTM elevation measurement does not correspond to the top of the canopy because radar scattering occurs throughout the canopy and is therefore located at the interferometric phase center. We calibrated SRTM-L data empirically assuming the lidar measurement to be the true vegetation height. The SRTM-L versus lidar height measurements are plotted in Figures 4, 5, 6, 7, and 8. In addition to SRTM-L, we tested a spatially filtered version (i.e., SRTM-F). We obtained SRTM-F by adaptive filtering of the SRTM-L elevation data with a method similar to that of Lee (1986), where we simply used an additive noise model. The adaptive filter preserves spatial resolution, thus edges, while reducing additive noise in regions with variance less then a user defined σ_h^2. We modeled the noise level σ_h as the Root Mean Square Error (RMSE) of the lidar versus SRTM-L regressions of Table 1 (i.e., σ_η = 1.8 m) and used a filter window of 0.9 ha (5 × 5 pixels) to preserve sharp tree height edges that are characteristic of the mangrove forests. Larger windows could be used to reduce noise further, but transitions between tall and scrub mangroves then become blurred (i.e., loss of spatial resolution). Spatial filtering had two effects: the first was a slight improvement of the height estimation and the second was the conversion of the SRTM-L integer data into a continuous height estimate (floating point) as shown in Figure 8b. We refer to the filtered SRTM-L data as SRTM-F.

We fitted a linear and a quadratic regression curve to each transect individually. The linear and quadratic regressions had similar RMSE. However, a single linear regression did not fully capture the difference in slope between tall and short mangroves; the slope was around 0.77 for the three western lidar transects and 0.47 for the scrub mangrove transect in Taylor Slough. The use of separate linear functions would have required setting a threshold based on the scrub mangrove polygons from the UG land-cover map for which we found the mean SRTM-L elevation and standard deviation to be 3.2 m and 1.3 m, respectively. The quadratic regressions for SRTM-L and SRTM-F are given in Table 3 with RMSE of 2.1 m and 2.0 m, respectively.

In order to estimate mean tree height from SRTM-F, we used the quadratic relation between lidar and SRTM (i.e., Table 3: Filtered and also shown in Figure 8b) to capture

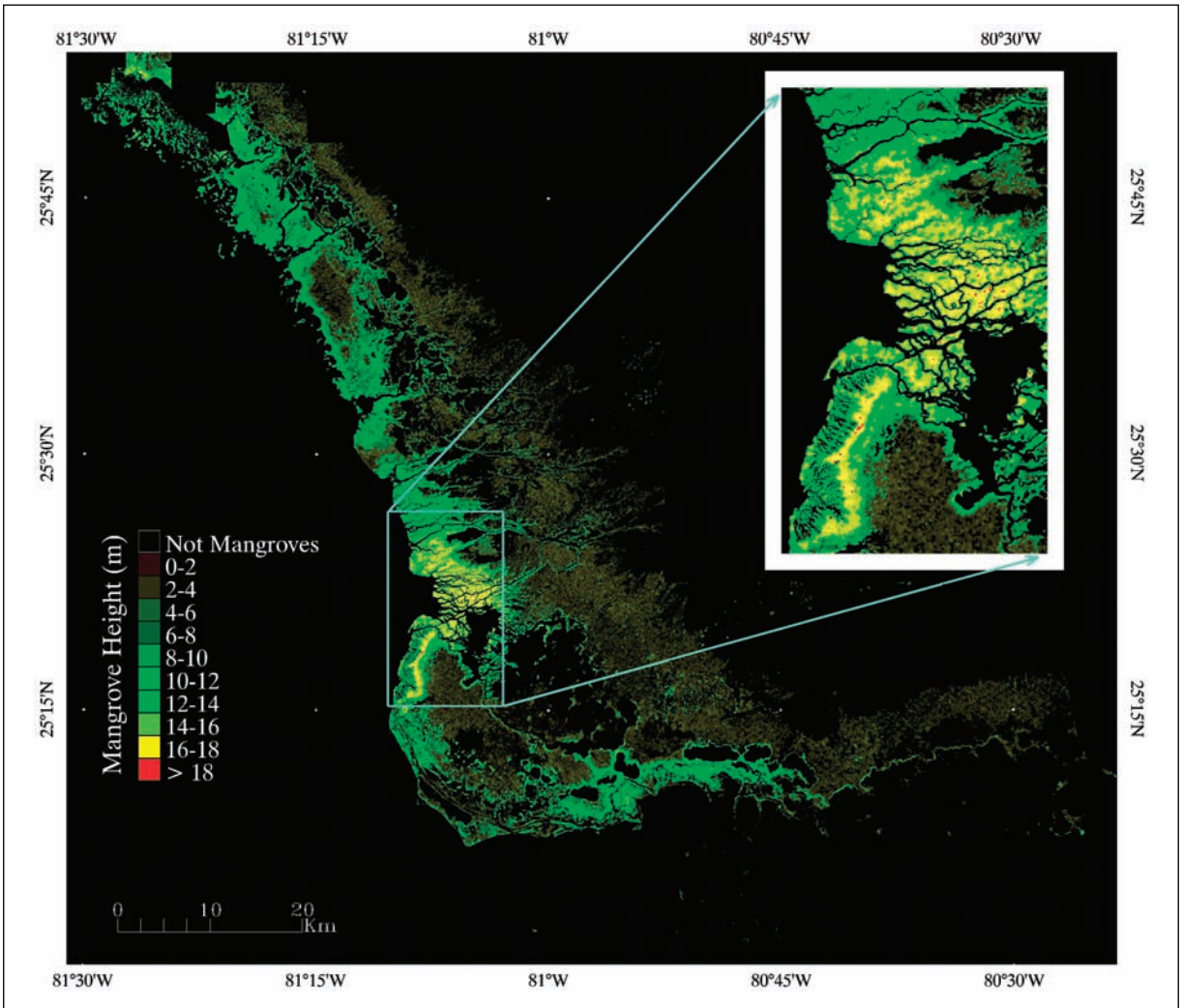

Plate 2. Map of mangrove mean tree height for the Everglades National Park, south Florida. The RMSE estimation error is 2 m per pixel. This map shows that most tall mangroves are found along the west coast along several tidal creeks (fringe forest), particularly around the mouth of the Shark River (Latitude 25° 21′N and Longitude 81° 7′W). Along this height gradient, basin and scrub forests are very distinct in their landscape position, with the latter category widely distributed more inland.

the trends reducing calibration of SRTM to a single function. We first applied the mangrove mask to select and isolate mangrove regions and then applied the quadratic regression (Table 3: Filtered) to obtain the *enhanced* SRTM (SRTM-E) map which contains only the mangrove areas (Plate 2).

SRTM-E (Plate 2) is the first published 3D view of the mangroves of ENP; this map shows that most tall mangroves are found along the west coast along several tidal creeks (fringe forest), particularly around the mouth of the Shark River (Latitude 25° 21′N and Longitude −81° 7′W). Along this height gradient, basin and scrub forest are very distinct in their landscape position, with the latter category widely distributed more inland. Figure 9 shows the frequency distribution of mangrove height within Everglades National Park, indicating that most of the mangrove region is in the scrub category (Lugo and Snedaker, 1974) less than 2 m in height.

Biomass Estimation

Because there are no specific allometric equations published for the ENP sites to estimate biomass, we used published allometric equations obtained for mangrove forest in neotropical sites (Fromard *et al.*, 1998; Ross *et al.*, 2001). In each study site we measured individual tree diameter at breast height (DBH) and identified the species. Our method for estimating tree biomass/plot biomass at the Shark, Broad, and Harney River sites and the Biscayne National Park sites is summarized in Table 4. In brief, we applied allometric equations published by Fromard *et al.* (1998) along with biomass relationships from a previous study conducted in the Biscayne Bay Coastal Wetlands in Biscayne National Park (see Ross *et al.*, 2001). In Biscayne National Park, biomass of stems <2 m in height and <1 cm DBH along with stems 1 to 5 cm DBH (for all sites) were calculated by assuming the mean stem biomass within six categories (<30 cm ht, 30 to 60 cm ht, 60 to 100 cm ht, 100 to 200 cm ht, 1 to 5 cm DBH, and >5 cm DBH) in an existing database from Biscayne National Park (Ross *et al.* 2001). For *Rhizophora* and *Avicennia* trees >5 cm DBH, we applied allometric equations published by Fromard *et al.* (1998). However, because Fromard's *Laguncularia* equation were based on trees <10 cm DBH, we applied his regression for *Rhizophora* to all *Laguncularia* individuals

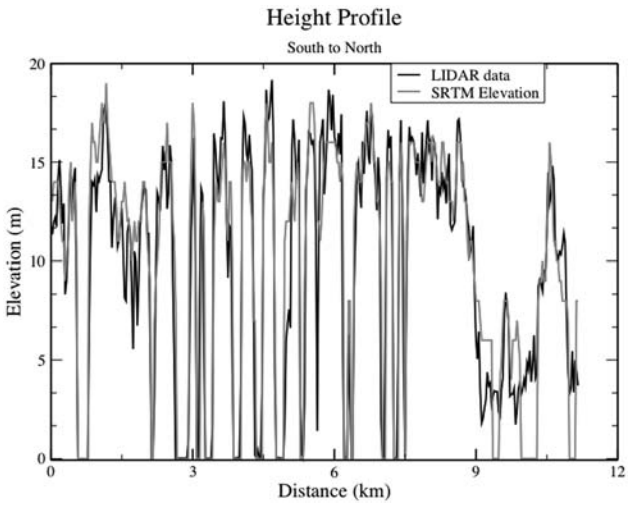

Figure 5. The North-South Transect: (a) Elevation profile for the lidar and SRTM data along the transect going toward the north. The profile is single valued at each point and therefore may not be representative of local statistics. (b) SRTM-L elevation versus lidar elevation. We fitted a linear and a quadratic regression curve given in Table 1 with correlation coefficients of 92 percent.

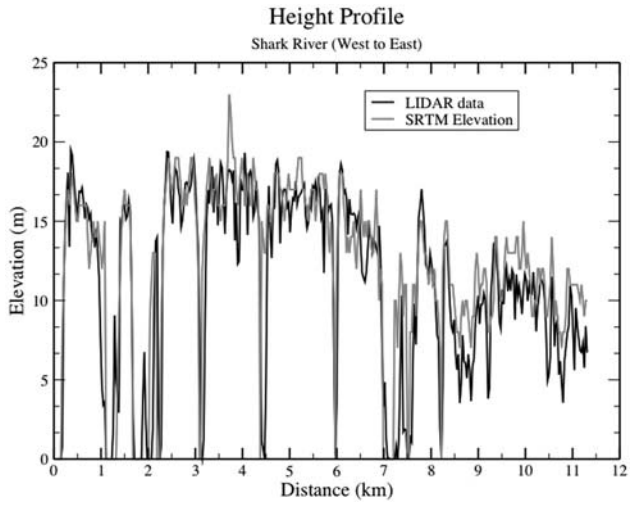

Figure 6. The Shark River Transect: (a) Elevation profile for the lidar and SRTM data along the Shark River. The profile is single valued at each point and therefore may not be representative of local statistics. (b) SRTM-L elevation versus lidar elevation. We fitted a linear and a quadratic regression curve given in Table 1 with correlation coefficients of 93 percent.

>10 cm diameter, which may cause a negligible overestimation in a few sites. For the few *Conocarpus erectus* stems sampled, we applied the *Laguncularia* biomass equations for each size class.

To derive a stand-level relationship between mean stem height (H) and biomass (B), we applied linear regression to data from 25 plots (22 from the transects and 3 were from Biscayne Bay). The resulting equation is B(Mg/ha) = 10H(m), with slope $m = 10$ with standard error $\sigma_m = 1.4$, and is illustrated with the stand data in Figure 10. The standard error σ_{Hf} of the field mean height H_f is negligible when assuming we measured heights of an average of 13 trees per site. For example, a 20 m tree has a 2 m field measurement standard error, thus computing the quadratic sum of error over 13 trees indicates a forest stand with $H_f = 20$ m has a standard error of 55 cm. Most of the biomass variation observed in Figure 10 may in fact be due to natural variability of stand height in the mangrove forest with a RMSE percent error of 0.37. The linear regression was applied directly to SRTM-E to map the mangrove standing biomass shown in Plate 3 (SRTM-BIOMASS).

We computed the SRTM-BIOMASS estimation standard error σ_B by propagating the errors from the regressions for SRTM-E mean tree height estimation error $\sigma_H = 2$ m (Figure 8b) and biomass field regression error $\sigma_M = 1.4$ m (Figure 10) such that: $\sigma_B = \sqrt{\left(\frac{\partial B}{\partial h}\right)^2 \sigma_h^2 + \left(\frac{\partial B}{\partial h}\right)^2 \sigma_m^2}$, which results in σ_B varying between ±20 Mg/ha for stands with $h = 1$ m to ±40 Mg/ha for $h = 25$ m (Figure 10).

In Figure 9, we show the frequency distribution of standing biomass as a function of stand mean tree height. It

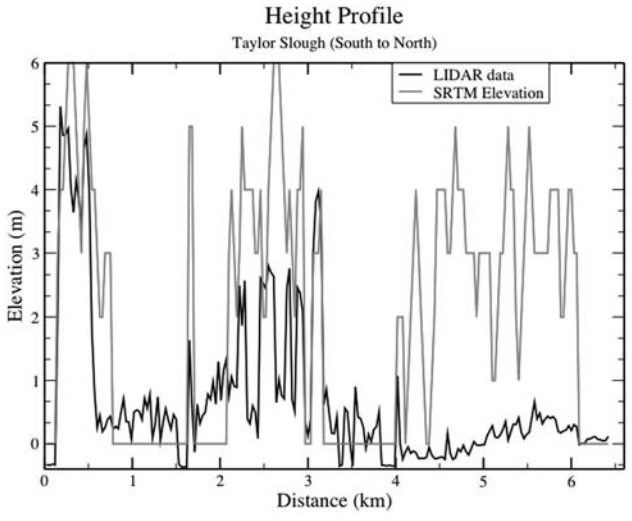

(a)

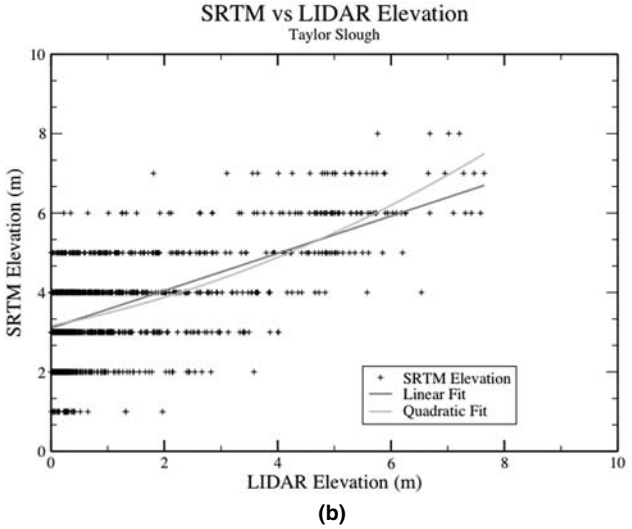

(b)

Figure 7. The Taylor Slough Transect: (a) Elevation profile for the lidar and SRTM data along the transect going toward the north. The profile is single valued at each point and therefore may not be representative of local statistics. The Taylor Slough is characterized by scrub mangroves spatially distributed in patches with height less then 2 m. (b) SRTM-L elevation versus lidar elevation. We fitted a linear and a quadratic regression curve given in Table 1 with correlation coefficients 51 percent and 58 percent, respectively.

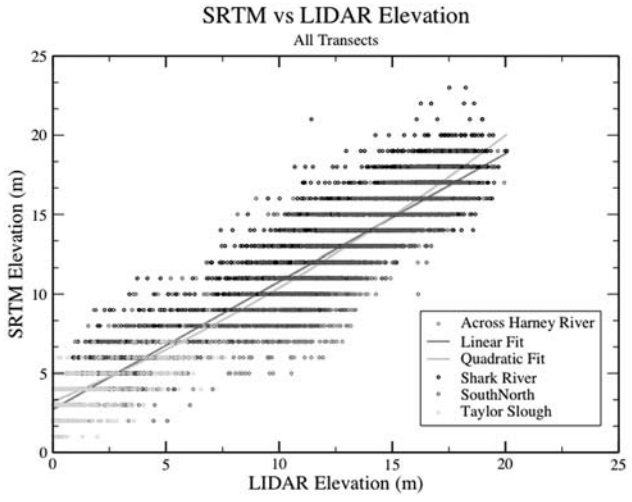

(a)

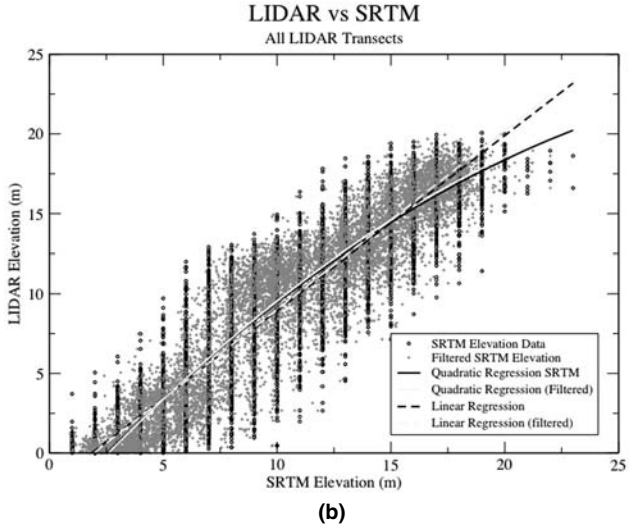

(b)

Figure 8. (a) All transect data are shown on this plot along with the linear and quadratic regression fits given in Table 1. Every fit has a 93 percent correlation. Although similar error are found for both fits, the quadratic fit seems to best capture the apparent scrub and tall mangrove regimes switching at around $H_{\text{lidar}} = 7.5$ m. Using only the mangroves with $H_{\text{lidar}} > 7.5$, the slope becomes 0.94. (b) This figure shows the opposite relation where the lidar elevation is plotted against SRTM Elevation. We plotted the SRTM data only corrected for the ground elevation (i.e., SRTM-L) as well as filtered version (i.e., SRTM-F). We fitted quadratic curves through both datasets as given in Table 2. We use the relation obtained from the enhanced SRTM dataset to estimate the mean tree height at each pixel.

shows that although most of the ENP mangroves are scrub forests, the standing biomass is concentrated in forest stands of intermediate height, i.e., approximately 8 m. The histogram standard error $\sigma_{\text{HistBiomass}}$ was again obtained by error propagation using σ_B and land cover error σ_{class}. Although we are confident the mangrove mask accurately (i.e., near 100 percent) represents the areas of tall mangroves that were visited during the field campaigns, we used $\sigma_{\text{class}} = 7.5$ percent, which takes into account both the mangrove commission and omission errors of the vegetation map. Using the SRTM-BIOMASS we estimated the total content of standing biomass in the mangroves of ENP to be 5.6×10^9 kg $\pm$ 0.1 $\times 10^9$ kg. The small estimation error assumes each SRTM-E height measurement is independent and considers σ_{class} of the mangrove mask.

Conclusion

We produced a map of mean mangrove height for the entire Everglades National Park using Shuttle Radar Topography

TABLE 2. REGRESSION FITS FOR HSRTM AGAINST H_{LIDAR} FOR THE FOUR INDIVIDUAL LIDAR TRANSECTS AS WELL AS FOR THE OVERALL TRANSECTS. SRTM ELEVATION IS FOUND TO VARY BY LESS THEN 1.8 M AROUND THE LIDAR ESTIMATED HEIGHT

LIDAR Transect	Regression Function	RMSE (m)
Shark River	$H_{srtm} = 4.21 + 0.78\ H_{lidar}$	1.51
	$H_{srtm} = 2.94 + 0.096\ H_{lidar} - 0.015\ H_{lidar}^2$	1.46
South-North	$H_{srtm} = 3.16 + 0.77\ H_{lidar}$	1.55
	$H_{srtm} = 3.63 + 0.64\ H_{lidar} + 0.0064\ H_{lidar}^2$	1.55
Harney River	$H_{srtm} = 3.16 + 0.77\ H_{lidar}$	1.63
	$H_{srtm} = 3.63 + 0.64\ H_{lidar} + 0.0064\ H_{lidar}^2$	1.62
Taylor Slough	$H_{srtm} = 3.11 + 0.47\ H_{lidar}$	1.04
	$H_{srtm} = 3.16 + 0.28\ H_{lidar} + 0.037 * H_{lidar}^2$	1.03
All Transects	$H_{srtm} = 3.02 + 0.79\ H_{lidar}$	1.82
	$H_{srtm} = 3.34 + 0.64\ H_{lidar} + 0.01\ H_{lidar}^2$	1.80
	$H_{lidar} > 7.5$m case: $H_{srtm} = 0.89 + 0.94\ H_{lidar}$	1.80

TABLE 3. REGRESSION FITS FOR H_{LIDAR} AGAINST H_{SRTM}. THE ERROR IS SLIGHTLY LOWER WHEN THE SRTM ELEVATION DATA IS PROCESSED WITH THE ADAPTIVE FILTER. WE USE THE QUADRATIC FUNCTION DERIVED FOR THE FILTERED CASE TO ESTIMATE MANGROVE FOREST HEIGHT FROM SRTM ELEVATION DATA IN EVERGLADES NATIONAL PARK

SRTM data	Regression Function	RMSE (m)
SRTM-L	$H_{lidar} = -3.73 + 1.53 * H_{srtm} - 0.021\ H_{srtm}^2$	2.1
	$H_{lidar} = -2.04 + 1.10\ H_{srtm}$	2.2
SRTM-F (Filtered)	$H_{lidar} = -3.90 + 1.56\ H_{srtm} - 0.022\ H_{srtm}^2$	2.0
	$H_{lidar} = -2.19 + 1.12\ H_{srtm}$	2.0

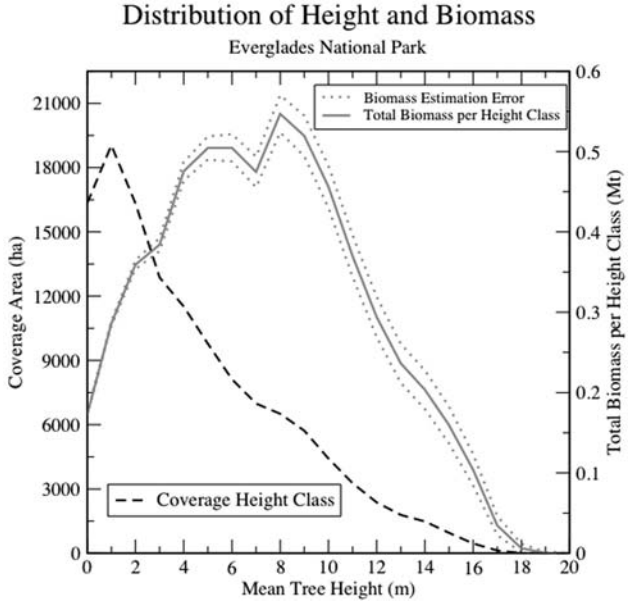

Figure 9. Coverage (hectares) of mean tree height (black) and distribution of total biomass (Mt = 10^9kg) as a function of mean tree height (gray). Although the Everglades National Park is mainly covered by scrub trees, the bulk of the biomass is contained in the medium-size mangrove forests.

TABLE 4. ALLOMETRIC EQUATIONS (FORMARD ET AL., 1998) AND DATABASE (ROSS ET AL., 2001) USED TO CALCULATE BIOMASS AS A FUNCTION OF STAND MEAN HEIGHT. THE TREES ARE SEPARATED IN DBH (I.E., DIAMETER AT BREAST HEIGHT) CLASSES: <1 CM; 1–5 CM; >5 CM. THE BIOMASS OF THE TALLEST CLASS (>5 CM) IS DERIVED FROM THE ALLOMETRIC EQUATIONS OF FROMARD ET AL. (1998)

Biomass Calculation for Stems ≥ 1 cm DBH in kg:
1–5 cm DBH: mean calculated from L-31E data base.
RHIMAN: 1.740 kg
LAGRAC: 8.416 kg
AVIGER: 3.251 kg
CONERE: 8.416 kg

≥5 cm DBH: allometric equations from Fromard 1998.
RHIMAN: $0.1282 * DBH^{2.6}$
AVIGER: $0.1400 * DBH^{2.4}$
LAGRAC & CONERE
5–10 cm DBH: $0.1023 * DBH^{2.5}$
>10 cm DBH: $0.1282 * DBH^{2.6}$ (same as for RHIMAN)

Biomass Calculations for Stems <2 m Height and <1 cm DBH in kg (means from L-31E data base):
For all stems <30 cm height (Scrub and Fringe (i.e. near the coast)):
RHIMAN: 0.003406 kg
LAGRAC: 0.001615 kg
AVIGER: 0.001301 kg
CONERE: 0.001615 kg

For Stems between 30 and 60 cm Height:

Species	Scrub	Fringe
RHIMAN	0.01845 kg	0.01421 kg
LAGRAC	0.00682 kg	0.00561 kg
AVIGER	0.00451 kg	0.00348 kg
CONERE	0.00369 kg	0.00561 kg

For Stems between 60 and 100 cm .Height:

Species	Scrub	Fringe
RHIMAN	0.06634 kg	0.05891 kg
LAGRAC	0.03550 kg	0.03659 kg
AVIGER	0.00632 kg	0.01989 kg
CONERE	0.02136 kg	0.03659 kg

For Stems between 100 and 200 cm Height:

Species	Scrub	Fringe
RHIMAN	0.16190 kg	0.24083 kg
LAGRAC	0.09709 kg	0.12089 kg
AVIGER	0.08123 kg	0.08123 kg
CONERE	0.12089 kg	0.12089 kg

Mission elevation data. The map has a spatial resolution of 30 m and a height estimation RMS error $\sigma_H = 2$ m. We calibrated the SRTM ground elevation data with a USGS DEM and found an artifact due to ascending passes. We corrected this artifact by subtracting a 2 m plane from SRTM elevation data in the southeast region of south Florida. Since bare ground area to reference bare Earth elevation was not available, we estimated the sea surface height from the SRTM data. We found that SRTM elevation had a positive bias of 1.1 m with respect to sea level around ENP. However, the large elevation noise (2.8 m standard deviation) measured over the sea, in addition to the effect of tide (approximately 30 cm) on the SRTM product, results in uncertainty to the estimated 1.1 m bias.

Mangrove height was calibrated empirically with lidar data, and the result is thus independent of the estimation of the elevation bias. We used a quadratic regression fit to

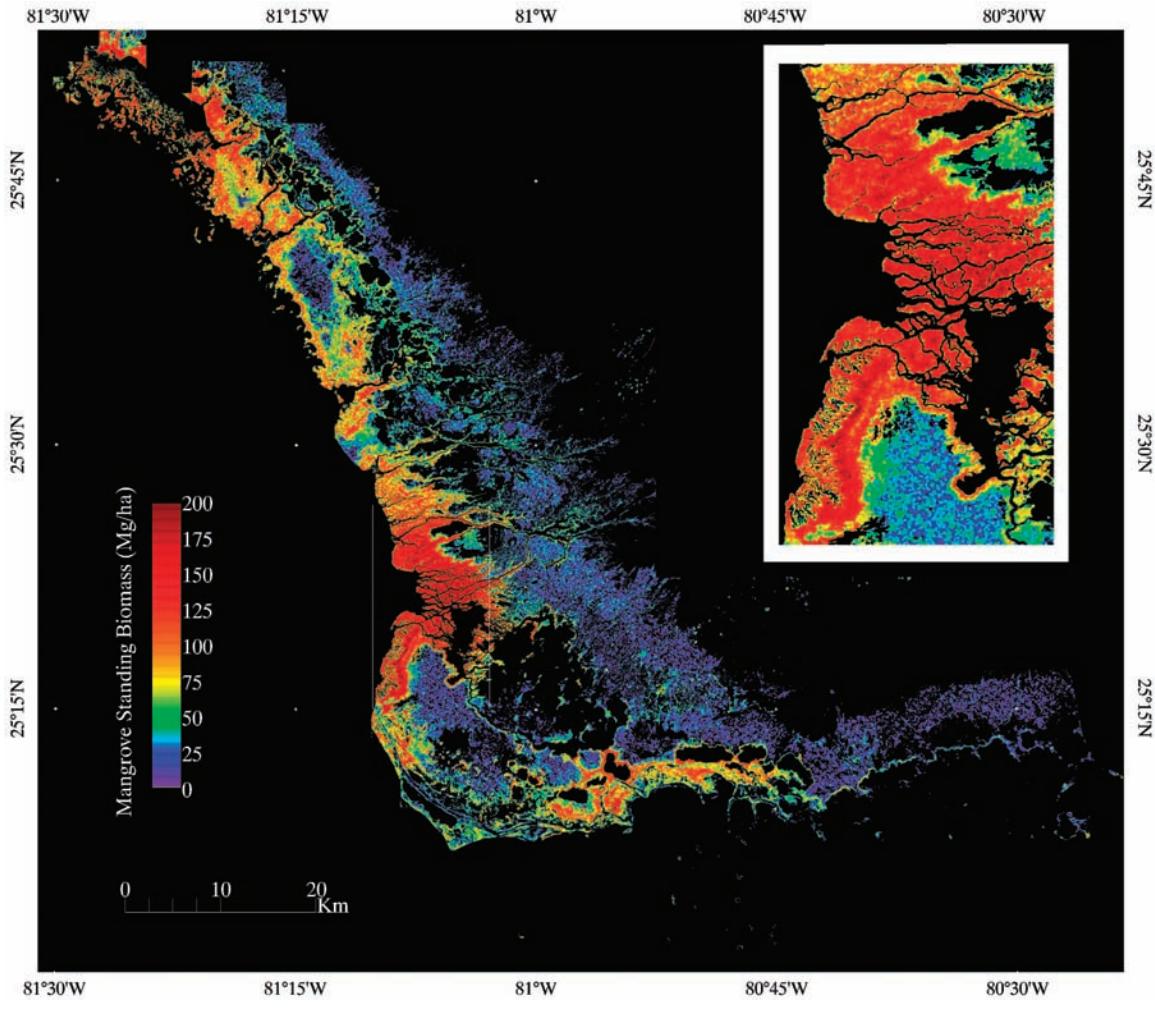

Plate 3. Map of standing biomass distribution (t/ha = Mg/ha) contained in mangroves of the Everglades National Park, south Florida. This map was computed using the mean tree height derived from SRTM elevation data (i.e., SRTM-E, Plate 2) and the linear regression for the biomass versus mean height (Figure 10).

follow the slope trends observed for fringe, basin, and scrub mangroves (Lugo and Snedaker, 1975). Using field data collected in ENP and Biscayne Bay, we derived a relationship for biomass versus stand mean tree height. This relationship was directly applied to the mean height map SRTM-E, to map the spatial distribution of mangrove biomass. Although most of the mangrove area in the ENP is dominated by scrub mangroves, the standing biomass in the mangroves of the Everglades mainly resides in the mid-size stands around 8 m in height. In addition, we estimated the total biomass of mangroves in the Everglades to be $5.6 \times 10^9 \pm 0.1 \times 10^9$ kg.

Although the main source of error in our analysis is the estimation of mean tree height using SRTM elevation data (σ_H = 2m), we found the quality of SRTM elevation data to be much better than the reported absolute 16 m accuracy (90 percent Linear Error). In order to improve the accuracy of SRTM mean tree height estimates, we would need to investigate the backscatter, single pass elevation (HH and VV) and interferometric correlation data. These SRTM datasets may carry useful information to identify and reduce and systematically quantify elevation error, but are not public. The second source of error, the linear regression between biomass and stand mean tree height, may potentially be improved by collecting additional field data, though we believe the dispersion due to natural variability is significant.

We showed that SRTM elevation can be used to estimate mangrove mean tree height and biomass accurately and could potentially be used to map mangrove forests around the world. Although the error is relatively small, it may not be sufficient for certain applications such as mapping of the Everglades grasslands and landscape modeling of sheet flows. In this work we used sea level as reference due to the lack of a possibly more accurate bare ground, a condition usually not found in tidal-dominated mangrove forests. In other regions, the tide range may reach several meters, and thus we could only rely on the knowledge of the geoid or field data.

Acknowledgments

The work presented in this paper was conducted by the Jet Propulsion Laboratory, California Institute of Technology, under contract with the National Aeronautics and Space Administration (NASA). This is an ongoing Interdisciplinary Science (IDS)

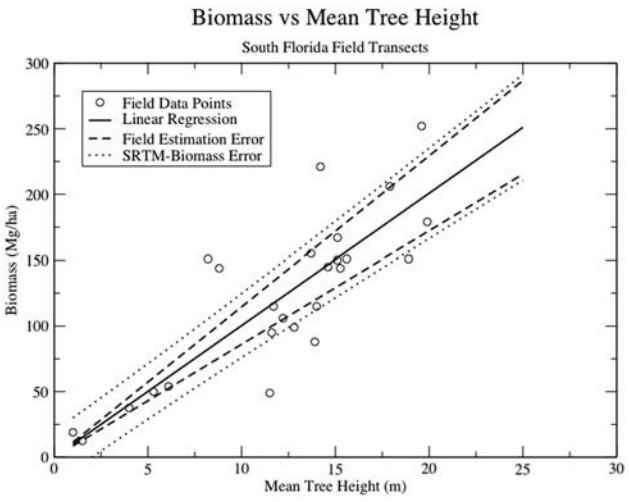

Figure 10. Biomass versus mean tree height as measured on the field and using allometric equations of Fromard *et al*. (1998) and databases of Ross *et al*. (2001). The linear regression is: Biomass (Mg/ha) = 10 * Height(m) with a correlation of 0.82 and RMS percent error of 37 percent.

project funded by NASA Land Cover Land Use Change program. This work was also partially funded by the National Science Foundation through the Florida Coastal Everglades Long-Term Ecological Research Program (DEB-9901514).

References

Alongi, D.M., 2002. Present state and future of the world's mangrove forests, *Environmental Conservation*, 29 (3):331–349.

Aschbacher, J., P. Tiangco, C.P. Giri, R.S. Ofren, D.R. Paudyal, and Y.K. Ang, 1995. Comparison of different sensors and analysis techniques for tropical mangrove forest mapping, *IGARSS Proceedings*, 3:2109–2111.

Badola R., and S.A. Hussain, 2005. Valuing ecosystem functions: An empirical study on the storm protection function of Bhitarkanika mangrove ecosystem, India, *Environmental Conservation*, 32(1):85–92.

Bourgeau-Chavez, L.L., K.B. Smith, S.M. Brunzell, E.S. Kasischke, E.A. Romanowicz, and C.J. Richardson, 2005. Remote monitoring of regional inundation patterns and hydroperiod in the greater everglades using synthetic aperture radar, *Wetlands* 25(1):176–191.

CERP, 2000. Comprehensive Everglades Restoration Plan, U.S. Army Corps of Engineer and South Florida Water Management District, Florida, URL: http://www.evergladesplan.org/, (last date accessed: 23 December 2005).

Cintron, G., and Y. Schaeffer-Novelli, 1984. Methods for studying mangrove structure, *The Mangrove Ecosystem: Research Methods* (S. C. Sneadaker and J. G. Sneadaker, editors), UNESCO, Paris, pp. 3–17.

Davis, S.E., J.E. Cable, D.L. Childers, C. Coronado-Molina, J.W. Day, C.D. Hittle, C.J. Madden, E. Reyes, D. Rudnick, and F. Sklar, 2004. Importance of storm events in controlling ecosystem structure and function in a Florida gulf coast estuary, *Journal of Coastal Research*, 20(4):1198–1208

Desmond, G., 2003. Measuring and mapping the topography of the Florida Everglades for ecosystem restoration, *GEER Conference, U.S. Geological Survey Greater Everglades Science Program: 2002 Biennial Report* (Open-File Report 03–54)

Fromard, F., H. Puig, E. Mougin, G. Marty, J.L. Betoulle, and L. Cadamuro, 1998. Structure, above-ground biomass and dynamics of mangrove ecosystems: New data from French Guiana, *Oecologia*, 115:39–53.

Gonneea M.E., A. Paytan, and J. Herrera-Silveira, 2004. Tracing organic matter sources and carbon burial in mangrove sediments over the past 160 years, *Estuarine Coastal and Shelf Science*, 61:211–227.

Grosenbaugh, L., 1952. Plotless timber estimates – new, fast, and easy, *Journal of Forestry*, 50:32–37.

Held, A., C. Ticehurst, L. Lymburner, and N. Williams, 2003. High resolution mapping of tropical mangrove ecosystems using hyperspectral and radar remote sensing, *International Journal of Remote Sensing*, 24(13):2739–2759.

Hensley, S., P. Rosen, and E. Gurrola, 2000. The SRTM topographic mapping processor, *Proceedings of IGARSS'2000* (3):1168–1170.

Hyyppa, J., H. Hyyppa, P. Litkey, X. Yu, H. Haggren, R. Petri, U. Pyysalo, J. Pitkanen, and M. Maltamo, 2004. Algorithms and methods of airborne laser scanning for forest measurements, *Proceedings of the ISPRS Working Group VIII/2 on Laser Scanners for Forest and Landscape Assessment*, Freiburg, Germany, XXXVI (8/W2).

Jennerjahn, T.C., and V. Ittekkot, 2002. Relevance of mangroves for the production and deposition of organic matter along tropical continental margins, *Naturwissenschaften*, 89:23–30.

Kasischke, E.S., K.B. Smith, L.L. Bourgeau-Chavez, E.A. Rmanowicz, S. Brunzell, and C.J. Richardson, 2003. Effects of seasonal hydrologic patterns in south Florida wetlands on radar backscatter measured from ERS-2 SAR imagery, *Remote Sensing of Environment*, 88:423–441.

Kellndorfer, J., W. Walker, L. Perce, C. Dobson, J.A. Fites, C. Hunsaker, J. Vona, and M. Clutter, 2004. Vegetation height estimation from Shuttle Radar Topography Mission and National Elevation Datasets, *Remote Sensing of Environment*, 93:339–358.

Kovacs, J.M., J.F. Wang, and F. Flores-Verdugo, 2005. Mapping mangrove leaf area index at the species level using IKONOS and LAI-2000 sensors for the Agua Brava Lagoon, Mexican Pacific, *Estuarine Coastal and Shelf Science* 62:377–384.

Laba, M., S.D. Smith, and S.D. Degloria, 1997. Landsat-based land cover mapping in the lower Yuna River watershed in the Dominican Republic, *International Journal of Remote Sensing*, 18(14):3011–3025.

Lee, J.S., 1986. Speckle suppression and analysis for SAR images, *Optical Engineering*, 25(5):636–643.

Light, S.S., and J.W. Dineen, 1994, Water control in the Everglades: A historical perspective, *The Everglades—The Ecosystem and its Restoration* (S.M. Davis, and J.C. Ogden, editors), St. Lucie Press, Delray Beach, Florida, pp. 47–84.

Lucas, R.M., A.K. Milne, A. Mitchell, B. Donnelly, and J. Ellison, 2000. Use of stereo aerial photography for assessing changes in the extent and height of mangrove canopies in tropical Australia, *IGARSS Proceedings*, 5:1880–1882.

Lugo, A.E., and S.C. Snedaker, 1974. The ecology of mangroves, *Annual Review of Ecology and Systematics*, 5:39–65.

Lynch J.C., J.R. Meriwether, B.A. McKee, F. Vera-Herrera, and R.R. Twilley, 1989. Recent accretion in mangrove ecosystems based on 137Cs and 210Pb, *Estuaries*, 12:284–299.

McIvor, C.C., J.A. Ley, and R.D. Bjork. 1994. Changes in freshwater inflow from the Everglades to Florida Bay including effects on biota and biotic processes: A review, *The Everglades: The Ecosystem and Its Restoration* (S.M. Davis and J.C. Ogden, editors), Delray Beach, Florida, St. Lucie Press.

Mougin, E., C. Proisy, G. Marty, F. Fromard, H. Puig, J.L. Betoulle, and J.P. Rudant, 1999. Multifrequency and multipolarisation radar backscattering from mangrove forests, *IEEE Transactions on Geoscience and Remote Sensing*, 37(1):94–102.

PE&RS, 1999. Special Issue: The South Florida Vegetation Mapping Project, *Photogrammetric Engineering & Remote Sensing*, 65(2).

Proisy, C., E. Mougin, and F. Fromard, 1996. Investigating correlations between radar data and mangrove characteristics, *Proceedings IGARSS*'96, 1:733–735.

Proisy, C., E. Mougin, F. Fromard, and M.A. Karam, 2000. Interpretation of polarimetric radar signatures of Mangrove forests, *Remote Sensing of Environment*, 71:56–66.

Ramsey III, E.W., and J.R. Jensen, 1996. Remote sensing of mangrove wetlands: Relating canopy spectra to site-specific data, *Photogrammetric Engineering & Remote Sensing*, 62(8):939–948.

Rasolofoharinoro, M., F. Blasco, M.F. Bellan, M. Azipuru, T. Gauquelin, and J. Denis, 1998. A remote sensing based methodology for mangrove studies in Madagascar, *International Journal of Remote Sensing*, 19(10):1873–1886.

Rivera-Monroy V.H, R. Twilley, E. Medina, E.B. Moser, L. Botero, A.M. Francisco, and E. Bullard, 2004. Spatial variability of soil nutrients in disturbed riverine mangrove forests at different stages of regeneration in the San Juan River Estuary, Venezuela, *Estuaries*, 27:44–57.

Ross, M.S., J.F. Meeder, J.P. Sah, P.L. Ruiz, and G.J. Telesnicki, 2000. The southeast saline Everglades revisited: 50 years of coastal vegetation change, *Journal of Vegetation Science*, 11(1):101–112.

Ross, M.S., P.L. Ruiz, G.J. Telesnicki, and J.F. Meeder, 2001. Estimating aboveground biomass and production in mangrove communities of Biscayne National Park, Florida (USA), *Wetlands Ecology and Management*, 9:27–37.

Rudnick, D., Z. Chen, D. Childers, J. Boyer, and T. Fontaine, 1999. Phosphorus and nitrogen inputs to Florida Bay: The importance of the Everglades watershed, *Estuaries* 22:398–416.

Simard, M., G. DeGrandi, S. Saatchi, and P. Mayaux, 2000. Mapping tropical coastal vegetation using JERS-1 and ERS-1 radar data with a decision tree classifier, *International Journal of Remote Sensing*, 23(7):1461–1474.

Sklar, F., C. McVoy, R. VanZee, D.E. Gawlik, K. Tarboton, D. Rudnick, and S. Miao. 2002. The effects of altered hydrology on the ecology of the Everglades, *The Everglades, Florida Bay, and Coral Reefs of the Florida Keys* (J.W. Porter and K.G. Porter, editors), Boca Raton, Florida, pp. 39–82.

Smith, T.J., III, M.B. Robblee, H.R. Wanless, and T.W. Doyle, 1994. Mangroves, hurricanes and lightning strikes, *BioScience*, 44:256–262.

Spalding, M., F. Blasco, and C. Field, 1997. *World Mangrove Atlas*, International Society for Mangrove Ecosystems, Okinawa, Japan.

Twilley, R.R., R.H. Chen, and T. Hargis. 1992. Carbon sinks in mangroves and their implications to carbon budget of tropical coastal ecosystems, *Water, Air and Soil Pollution*, 64:265–288.

Valiela, I., J.L. Bowen, and J.K. York, 2001. Mangrove forests: One of the world's threatened major tropical environments, *Bioscience* 51:807–815.

Vegetation Map, 1999. Vegetation Map and Digital Database of South Florida's National Park Service Lands, Florida Coastal Everglades Long Term Ecological Research (FCELTER), Florida, URL: http://fcelter.fiu.edu/gis/everglades_map/ (last date accessed: 23 December, 2005).

Wang, Y., and M.L. Imhoff, 1993. Simulated and observed L-HH radar backscatter from tropical mangrove forests, *International Journal of Remote Sensing* 14(15):2819–2828.

Wang, L, W.P. Sousa, P. Gong, and G.S. Biging, 2004. Comparison of IKONOS and QuickBird images for mapping mangrove species on the Caribbean coast of Panama, *Remote Sensing of Environment*, 91:432–440.

Walker, W.S., L.E. Pierce, J.M. Kellndorfer, M.C. Dobson, C.T. Hunsaker, and J.A. Fites, 2004. A comparison of forest canopy height estimates derived from SRTM and TOPSAR in the Sierra Nevada of California, *Proceedings of IGARSS'04*, 4:2336–2339.

Wdowinski, S., F. Amelung, F. Miralles-Wilhelm, T.H. Dixon, and R. Carande, 2004. Space-based measurements of sheet-flow characteristics in the Everglades wetland, Florida, *Geophysical Research Letters*, 31(15).

Welch, R., and M. Madden. 1999. Vegetation Map and Digital Database of South Florida's National Park Service Lands, *Final Report to the U.S. Department of the Interior, National Park Service, Cooperative Agreement Number 5280–4–9006*, Center for Remote Sensing and Mapping Science, University of Georgia, Athens, 44 p.

Woodroffe, C. 1992. Mangrove sediments and geomorphology, *Tropical Mangrove Ecosystems* (A.I. Robertson and D.M. Alongi, editors), *American Geophysical Union*, Washington, D.C., pp. 7–42.

Zhang, K., S.C. Chen, D. Whitman, M.L. Shyu, J.H. Yan, and C.C. Zhang, 2003. A progressive morphological filter for removing nonground measurements from airborne LIDAR data, *IEEE Transactions on Geoscience and Remote Sensing*, 41:872–882.